

Electronic Supplementary Information

Multifunctionalized zirconium-based MOF as a novel support for dispersed copper:

Application in CO₂ adsorption and catalytic conversion

Albert Rosado,^a Ioana-Maria Popa,^b Ahmad Abo Markeb,^{c,d} Javier Moral-Vico,^c Eva Maria Naughton,^f Hans-Georg Eckhardt,^f José A. Ayllón,^c Ana M. López-Periago,^a Concepción Domingo,^{a*} Leila Negahdar^{f*}

^a *Materials Science Institute of Barcelona, ICMAB-CSIC, Campus UAB s/n, 08193 Bellaterra, Spain. Email: conchi@icmab.es*

^b *Department of Chemistry, RWTH Aachen University, Aachen 52074, Germany*

^c *Department of Chemical, Biological and Environmental Engineering, UAB, Campus UAB s/n, 08193 Bellaterra, Spain.*

^d *Department of Chemistry, Faculty of Science, Assiut University, Assiut 71516, Egypt.*

^e *Department of Chemistry, UAB, Campus UAB s/n, 08193 Bellaterra, Spain.*

^f *School of Chemistry, University College Dublin, Belfield, Dublin 4, Ireland. Email: leila.negahdar@ucd.ie*

Table of contents

Experimental section	3
<i>Synthesis of H₄TBAPy-NH₂</i>	3
Figure S1. Schematic representation of H ₄ TBAPy-NH ₂ synthesis.	5
<i>Characterization of compounds 1, 2, 3 and 4 (H₄TBAPy-NH₂)</i>	5
Figure S2. ¹ H-NMR spectra of compound 1 in CDCl ₃ .	6
Figure S3. ¹ H-NMR spectra of compound 2 in CDCl ₃ .	6
Figure S4. ¹ H-NMR spectra of compound 3 in DMSO-d ₆ .	7
Figure S5. ¹ H-NMR spectra of compound 4 (H ₄ TBAPy-NH ₂) in DMSO-d ₆ .	7
<i>Electrocatalytic equipment and method</i>	8
Figure S6. Set-up for the electrochemical reduction of CO ₂ .	9
<i>Thermocatalytic equipment and method</i>	10
Figure S7. Schematic set-up used for the thermocatalytic reduction of CO ₂ .	11
Materials characterization	12
Figure S8. SEM micrograph of a single NU-1000-NH ₂ particle.	12
Figure S9. PXRD patterns of the studied samples.	12
Figure S10. ATR-FTIR spectra of the studied samples.	13
<i>Quantitative analysis of PrSH by ¹H-NMR</i>	14
Figure S11. ¹ H-NMR spectra of PrSH in DMSO-d ₆ .	14
Figure S12. ¹ H-NMR spectra of digested NU-1000-NH ₂ /PrSH in DMSO-d ₆ .	15
Figure S13. SEM image and EDS mapping of a NU-1000-NH ₂ /PrSH particle.	16
Figure S14. TGA analysis of the studied samples.	16
Figure S15. PXRD patterns of the studied samples at 2θ range from 2 to 100°.	17
Figure S16. Pore size distribution of the studied samples.	17
Figure S17. CO ₂ enthalpy of adsorption (Q _{st}) of the studied samples.	18
<i>Electrocatalysts characterization and results</i>	
Figure S18. PXRD patterns of the studied working electrodes.	19
Figure S19. SEM and EDS mapping of NU-1000-NH ₂ /PrS-Cu@support.	19
Figure S20. CV scans of @FTO samples.	20
Figure S21. NU-1000-NH ₂ /PrS-Cu@FTO image before and after reaction.	20
Figure S22. CV scans of @rGO samples.	21
Figure S23. CV scans of @rGO at different scan rates and derived results.	21
Figure S24. HPLC analysis of liquid electrocatalytic products.	22
Figure S25. Chronoamperometric measurements of @rGO at three potentials.	22
References	23

Experimental section

Synthesis of H₄TBAPy-NH₂

The synthetic steps for ligand preparation were slightly modified with respect to the original protocol,¹ and involved the synthesis of three intermediates and the final compound (Fig. S1). All the employed reactants, reagents and solvents for ligand synthesis were supplied by abcr.

Compound 1 was obtained by mixing 1.50 g (2.90 mmol) of 1,3,6,8-tetrabromopyrene, 4.40 g (17.35 mmol) of bis(pinacolato)diboron and 1.75 g (17.8 mmol) of anhydrous potassium acetate (KOAc) in a 100 mL Schlenk flask together with a magnetic stirrer. The flask was subjected to 5 cycles of Ar-vacuum previous to the addition of 30 mL of anhydrous dimethylsulfoxide (DMSO). The resulting crude was bubbled with Ar for 15 min while stirring. After this time, 0.18 g (0.25 mmol) of [1,1'-bis(diphenylphosphino)ferrocene]dichloropalladium(II) (Pd(dppf)Cl₂) were added under Ar atmosphere and the flask was subsequently covered with a septum poked with an Ar-filled balloon. The suspension was stirred at 500 rpm and heated to 85 °C for 2 days. Then, the brownish dispersion was poured into 450 mL of deionized H₂O and filtered by suction. The product was further washed with distilled H₂O and methanol (*ca.* 500 mL MeOH) until the filtrate got clear. Finally, the solid was suspended in a mixture of dichloromethane:methanol (DCM:MeOH, 25:75 mL) and filtered by suction to afford compound **1** (77% yield). ¹H-NMR (300 MHz, chloroform-d, CDCl₃) shift (ppm): 9.18 (s, 4H), 9.00 (s, 2H), 1.52 (s, 48H) (Fig. S2).

Compound 2. 2 g (2.83 mmol) of compound **1**, 3.40 g (12.5 mmol) of ethyl 4-bromo-3-nitrobenzoate, 4.70 g (34.0 mol) of potassium carbonate (K₂CO₃) and 0.30 g (0.26 mmol) of tetrakis(triphenylphosphine)palladium(0) (Pd(PPh₃)₄) were placed into 100 mL Schlenk flask together with a magnetic stirrer. The flask was submitted to 5 cycles of Ar-vacuum previous to the addition of 50 mL of deoxygenated dioxane (formerly bubbled with N₂ for 30 min while stirring). The flask was stirred at 500 rpm and heated to 90 °C under Ar atmosphere for 4 days. After this time, dioxane was removed by rotary evaporation and 50 mL of deionized H₂O were added to the resulting crude. The suspension was extracted with DCM until the organic phase was clear. The collected organic fractions were dried over anhydrous sodium sulfate (Na₂SO₄) and filtered through Celite. Finally, the filtrate was concentrated to 5 mL by rotary evaporation and 100 mL MeOH were added to promote the precipitation of the compound **2** (45% yield). ¹H-NMR (300 MHz, CDCl₃) shift (ppm): 8.81 (m, 4H), 8.43 (m, 4H), 7.80 (m, 4H), 7.75 (m, 2H), 7.71 (m, 4H), 4.52 (q, 8H), 1.49 (t, 12H) (Fig. S3).

Compound 3. 2.70 g (2.75 mmol) of compound **2** and a magnetic stirring bar were placed into a 250 mL round bottom flask with 100 mL of tetrahydrofuran (THF). Then, 10.8 g (184 mmol, large excess) of Raney-Ni were added with the aid of 20 mL of THF. To the stirred mixture, 2.20 mL (44.0 mmol) of hydrazine mono hydrate were poured dropwise. The system was stirred at 500 rpm and refluxed at 80 °C for 4 h. After this time, the hot content was filtered and the collected solid was washed with ethyl acetate (EtOAc) and DCM (*note: do not let the solid dry in air since it is pyrophoric*). The filtrate was concentrated by rotary evaporation. Finally, the solid was suspended in a mixture of EtOAc:hexane (100:100 mL) and filtered by suction to yield compound **3** (55% yield). ¹H-NMR (300 MHz, DMSO-d₆) shift (ppm): 7.77 (m, 6H), 7.51 (m, 4H), 7.27 (m, 8H), 5.02 (m, 8H), 4.34 (q, 8H), 1.35 (t, 12H) (Fig. S4).

Compound 4. 0.80 g (0.94 mmol) of compound **3** and a magnetic stirring bar were placed into a 250 mL round bottom flask with 50 mL THF. Separately, 2 g (36 mmol) of potassium hydroxide (KOH) were dissolved in 36 mL of deionized H₂O. The KOH solution was added dropwise to the flask while stirring. The system was stirred at 500 rpm and refluxed at 80 °C overnight. After this time, the THF was removed by rotary evaporation. Then, 100 mL of deionized H₂O were added to solubilize the product and the resulting solution was filtered to remove any impurity. Finally, hydrochloric acid (HCl) 6 M was added dropwise until the formation of a yellowish precipitate, which was filtered to afford compound **4**, designated as H₄TBAPy-NH₂ (83% yield). ¹H-NMR (300 MHz, DMSO-d₆) shift (ppm): 12.72 (b, 4H), 7.78 (m, 6H), 7.49 (m, 4H), 7.25 (m, 8H), 5.01 (m, 8H) (Fig. S5).

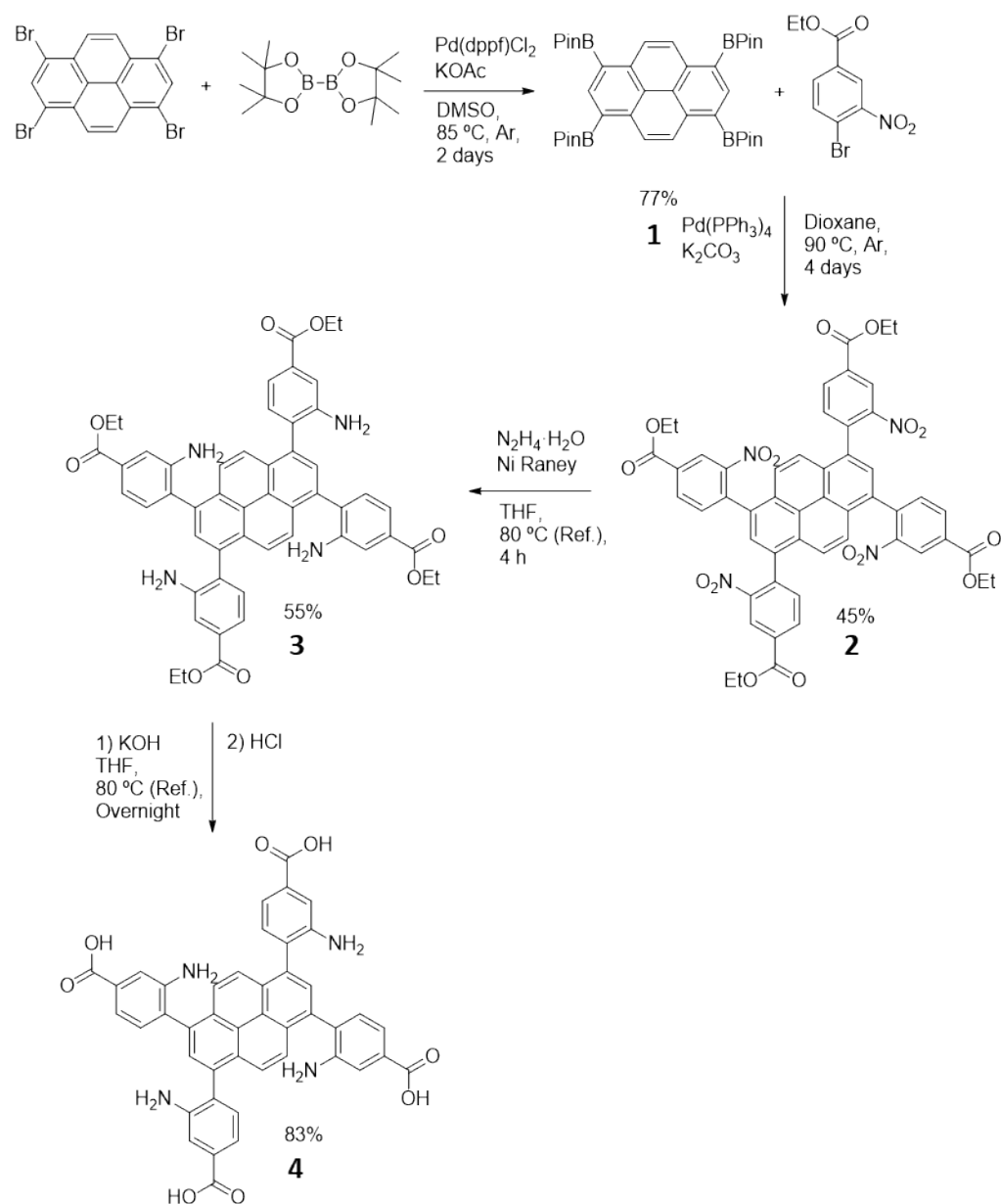


Figure S1. Schematic representation of the followed steps to synthesize compound **4** (H₄TBAPy-NH₂).

Characterization of compounds **1**, **2**, **3** and **4**

Proton nuclear magnetic resonance (¹H-NMR, Bruker Advance NEO 300 MHz) was used to ascertain the chemical structure of the synthesized organic ligand H₄TBAPy-NH₂ and intermediates, dissolved either in CDCl₃ or DMSO-d₆. In each case, recorded ¹H-NMR spectra matched data of published similar compounds (Fig. S2,3,4,5).

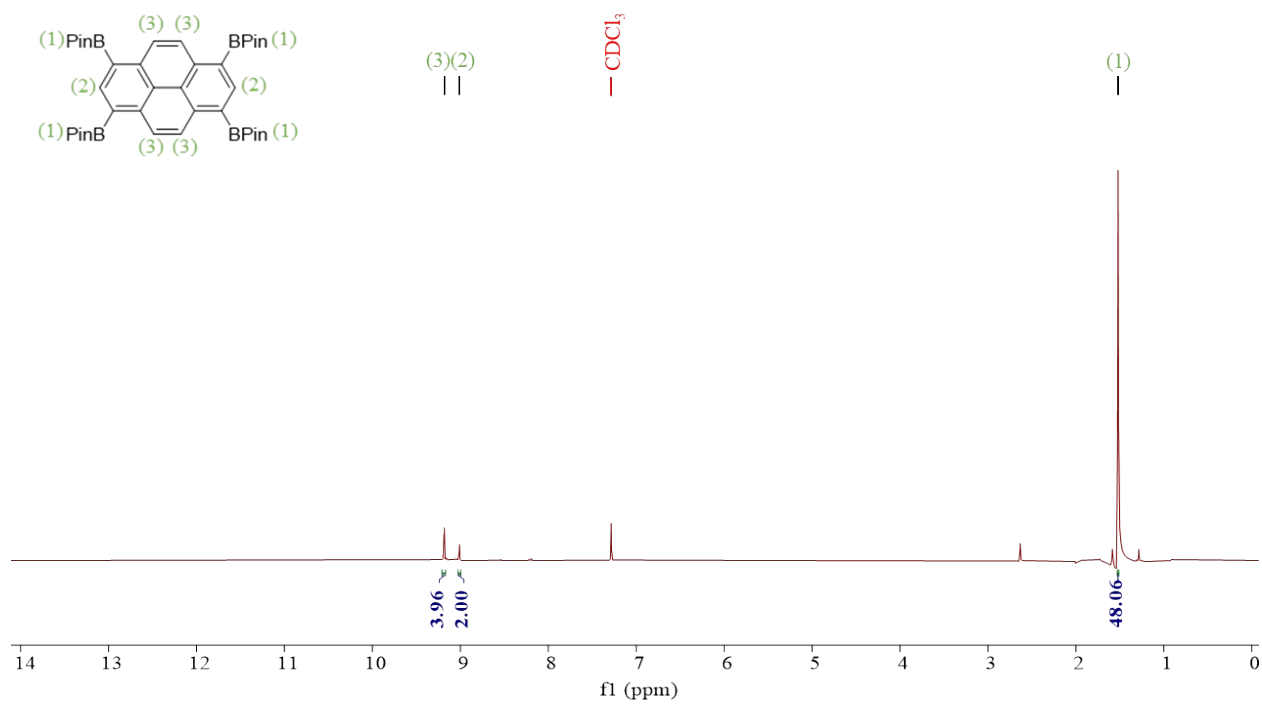


Figure S2. ¹H-NMR spectra of compound **1** in CDCl₃.

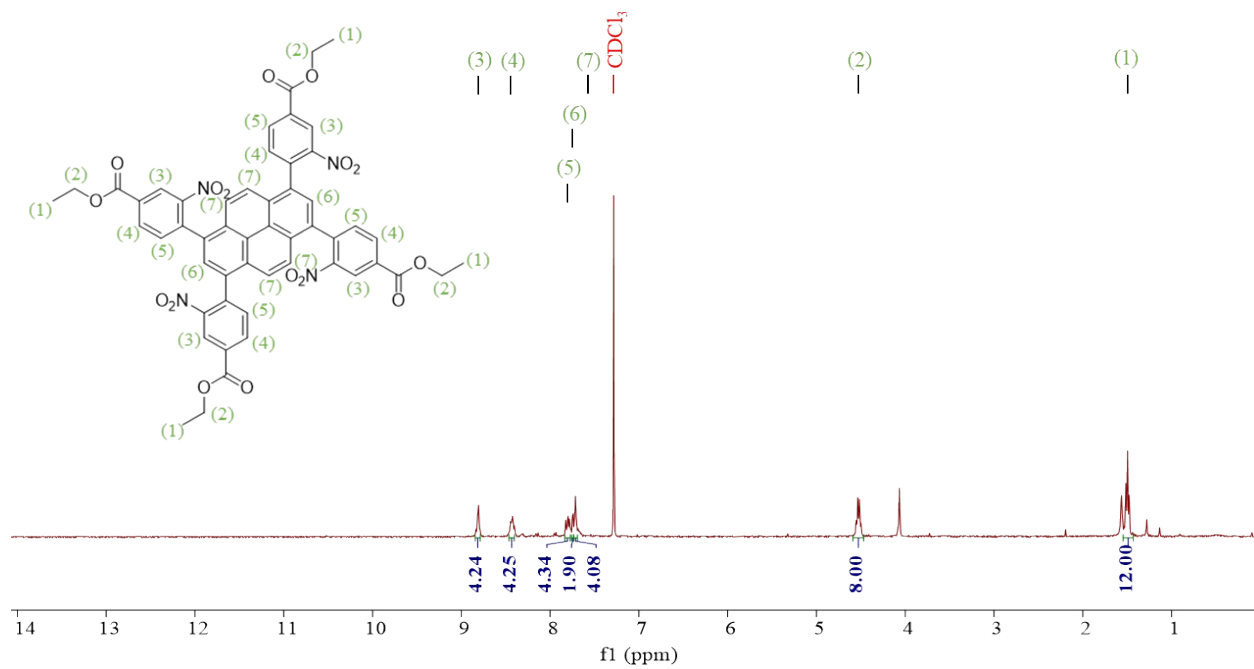


Figure S3. ¹H-NMR spectra of compound **2** in CDCl₃.

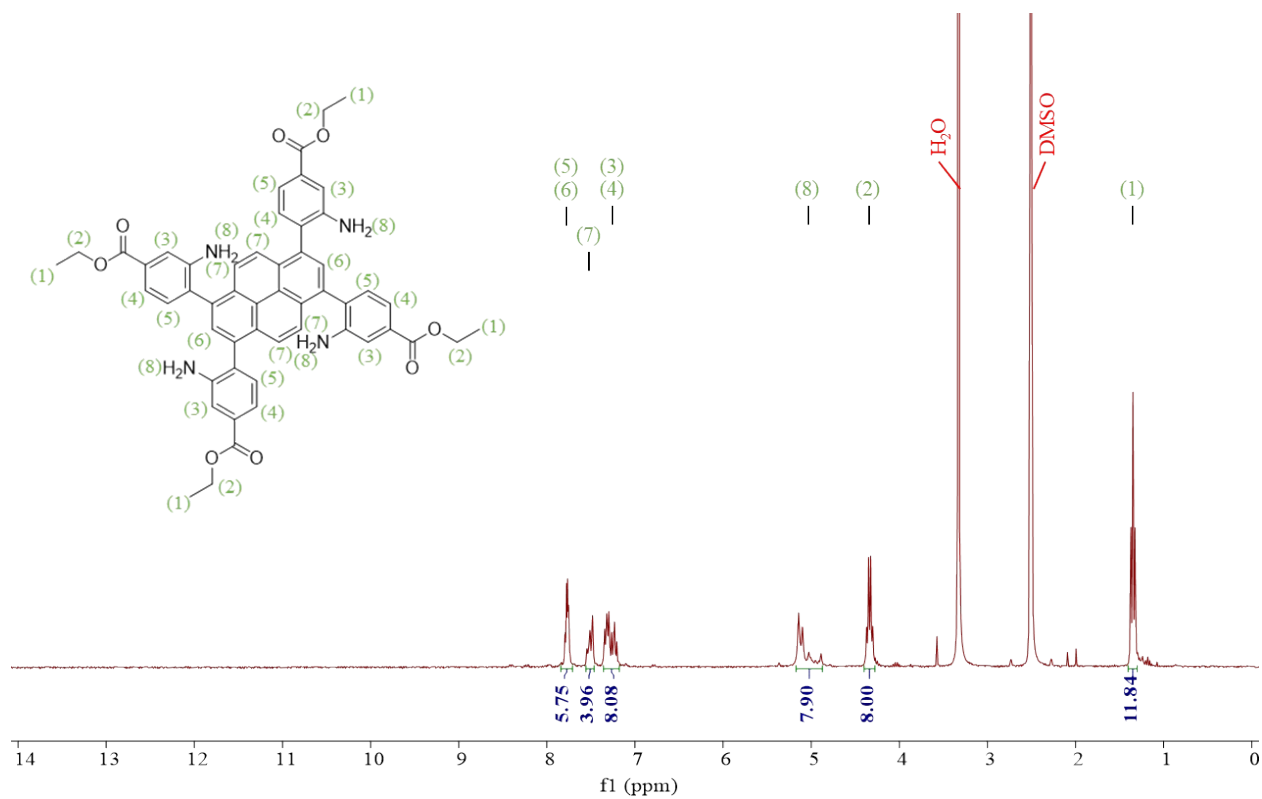


Figure S4. $^1\text{H-NMR}$ spectra of compound **3** in DMSO-d_6 .

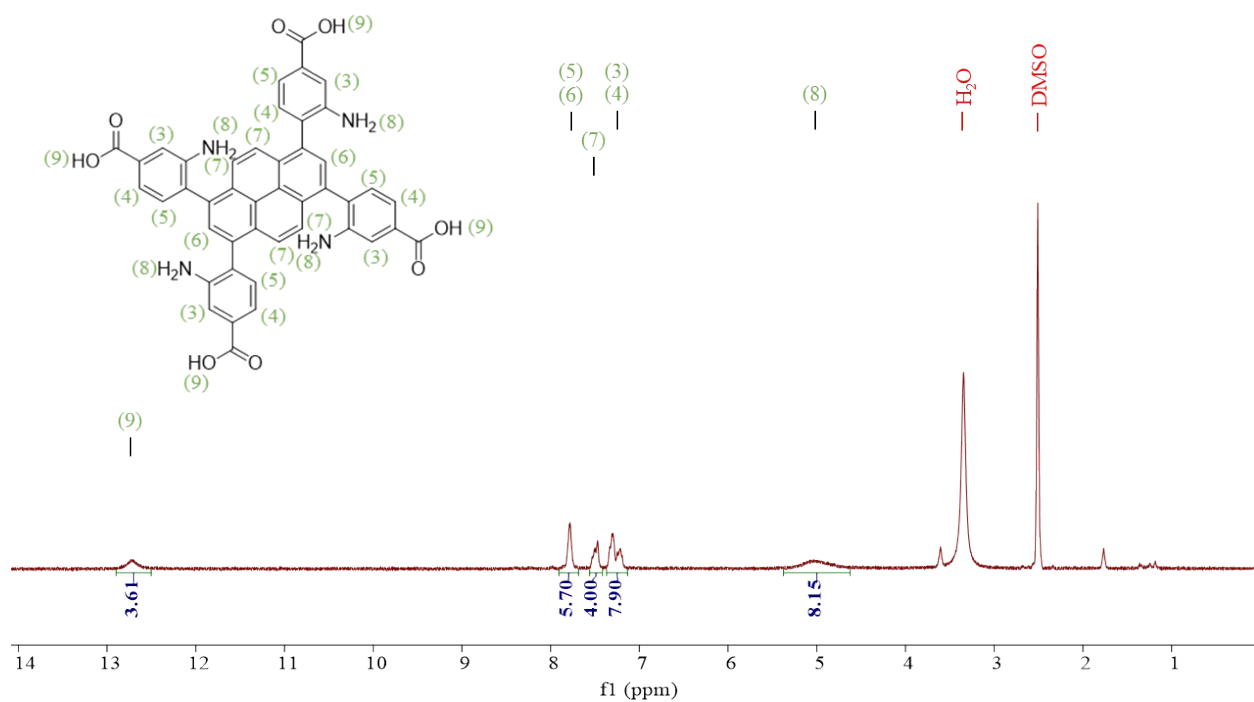


Figure S5. $^1\text{H-NMR}$ spectra of compound **4** ($\text{H}_4\text{TBAPy-NH}_2$) in DMSO-d_6 .

Electrocatalytic equipment and method

The electrocatalytic experiments were performed in a one-pot home-made cell divided into the anodic and cathodic spaces by placing an anionic exchange membrane in the middle (Fig. S6). All the electrochemical measurements were carried out using a Metrohm Autolab potentiostat PGSTAT101 (software Nova 2.1.6). The cell was filled with 40 mL of electrolyte of either 0.1M NaClO₄ with a pH of 5.46 or 0.1 M of KHCO₃ with pH of 6.80. A Pt sheet with an area of 1 cm², serving as a counter electrode (CE), was immersed in the anodic space, and a Ag/AgCl reference electrode (RE) and the NU-1000-NH₂/PrS-Cu@support working electrode (WE) were introduced in the cathodic space. The WEs were partially covered with insulation tape, resulting in exposed areas of *ca.* 0.4 cm² for @FTO and @rGO. Prior to start with the experiments, the system was purged by bubbling the electrolyte with N₂ for 20 min at a flow rate of 50 mLmin⁻¹. Once inert atmosphere was attained, an electrochemical pre-treatment was performed on the WEs by applying -0.6 V *vs* RHE for 10 min, in order to ensure the reduction of any copper species possibly reoxidized during manipulation. Then, CO₂ was bubbled in the solution at a flow rate of 50 mLmin⁻¹ until constant pH, confirming the saturation of the electrolytes. At this point, the electrocatalytic set-up was ready for the catalytic tests. In a typical experiment, a specific potential (from -0.4 to -1.6 V *vs* RHE) was applied for at least 1 h while keeping the CO₂ bubbling in the cathodic space. Gas and liquid aliquots were collected every 20 min through a small septum incorporated in the home-made lid. Gas aliquots were collected with a 500 μL gas-lock syringe and directly analysed in a Varian GC-450 gas chromatograph, equipped with a methaniser, TCD and FID detectors. Liquid aliquots were extracted with a syringe and stored for HPLC analysis. HPLC analysis was carried out in an Agilent 1200 reverse phase HPLC with an Automated Liquid Sampler (Agilent ALS G1329A), Thermostatted Column Compartment (Agilent TCC G1316A) Diode Array Detector (Agilent G1315D) and Refractive Index Detector (Agilent RID G1362A). The method details are as follow: Isocratic 0.005M H₂SO₄ in HPLC grade water (Sigma Aldrich 270733 - 2.5L) with a flow rate of 0.5 mL/min with a column temperature of 80 °C and RID temperature set to 55 degrees Celsius. The column is an Alltech OA-1000 Organic Acid Col. 300×6.5mm 9μm.

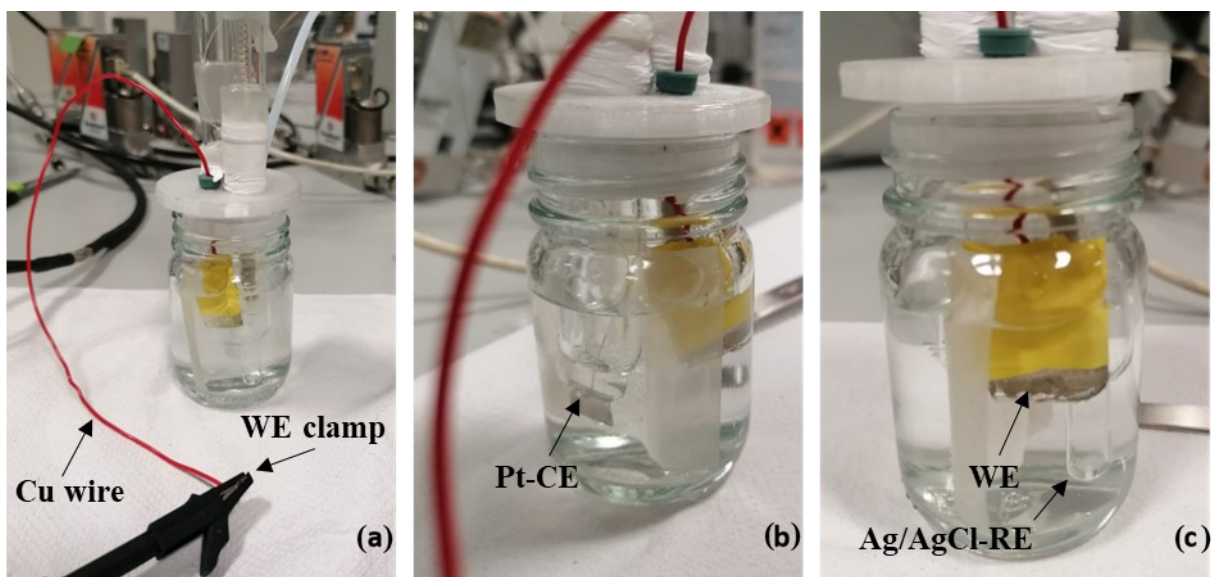


Figure S6. Set-up for the electrochemical reduction of CO_2 : (a) view of the entire one-pot system; (b) close-up view of the anodic space, showing the Pt-CE; c) close-up view of the cathodic space, showing the Ag/AgCl-RE and the WE with the exposed catalyst, connected through the copper wire (red) to the WE clamp (black).

Thermocatalytic equipment and method

Catalytic activity tests were carried out in a hand-made equipment settled by Process Integral Development Engineered & Tech. (Fig. S7). The equipment involves a pressurizer cylinder (1) loaded with H₂ or H₂:CO₂ (3:1) which, through an open/close valve (2) and a pressure regulator (3), deliver the gas mixture to the area in which the reaction takes place. The gas flow is regulated and measured by using a mass flow meter (4, Bronkhorst mini Cori-flow). The catalytic activity of the CO₂ hydrogenation was evaluated in a stainless steel fixed-bed reactor (5) with an internal diameter of 0.45 cm and a length of 9.00 cm. The reactor is connected to the system by two vespel and graphite ferrules and settled inside an oven of a 7890A Agilent gas chromatograph (6). The exhausted flow pass through a three-way needle valve (7) used to take aliquots at fixed periods of time in a sample bag (SKC FlexFoil PLUS Sample Bag). At the exit, a manometer (8) was used to measure system pressure and a ball valve to depressurize the system (9). First, sample was placed inside the fixed-bed tubular column and subjected to *in situ* reduction under H₂ flow (20 mLmin⁻¹) at 180 °C during 2 h. Catalytic reactions were then straightforward performed in the same fixed-bed tubular column, just by switching the flow of pure H₂ to a mixture of CO₂/H₂. The pressure and gas flow rate were set at 10 bar and 10 mLmin⁻¹, respectively. After the steady state was reached (*ca.* 20 min), ejected products were determined by collecting three aliquots at each settled temperature, from 180 to 280 °C. MeOH was measured using a Shimadzu GC-2010 gas chromatograph with a flame ionization detector and helium as a carrier gas. Data was analyzed with Chromeleon software (Version 6.80 SR5b). The inlet and the detector temperature were 260 °C and 280 °C respectively, and the inlet flow was 50 mLmin⁻¹. The amount of CO₂ and CO was quantified using an Agilent Tech. 7890B gas chromatograph with a thermal conductivity detector and helium as a carrier gas. OpenLab (Version A.01.04) was the software used, and the inlet temperature and flow were 120 °C and 20 mLmin⁻¹, respectively. The detector temperature was at 150 °C.

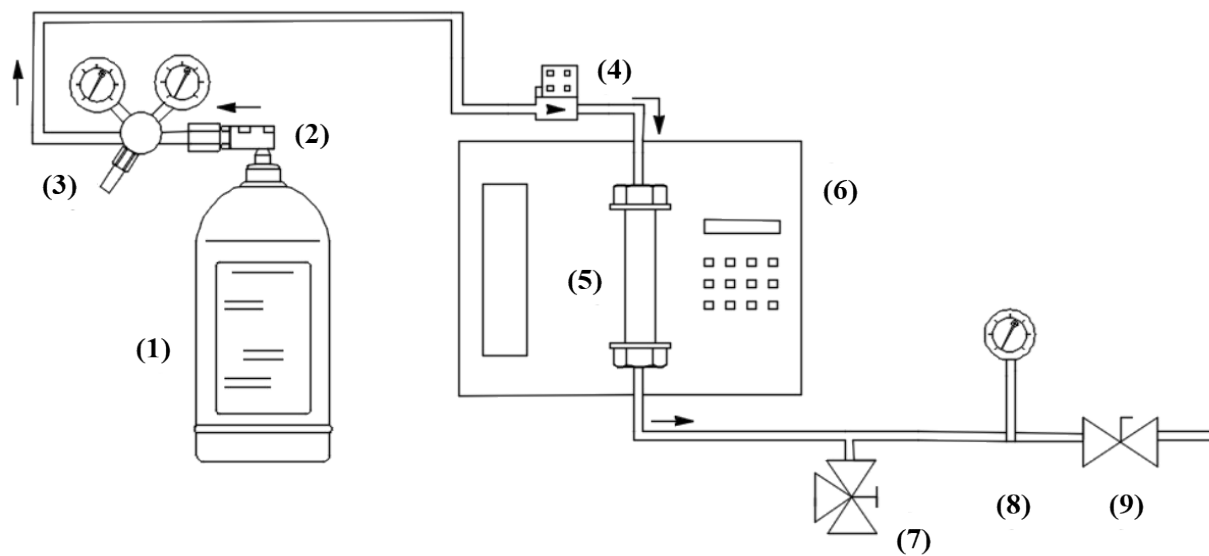


Figure S7. Schematic set-up used for the thermocatalytic conversion of CO₂ to MeOH.

Materials characterization

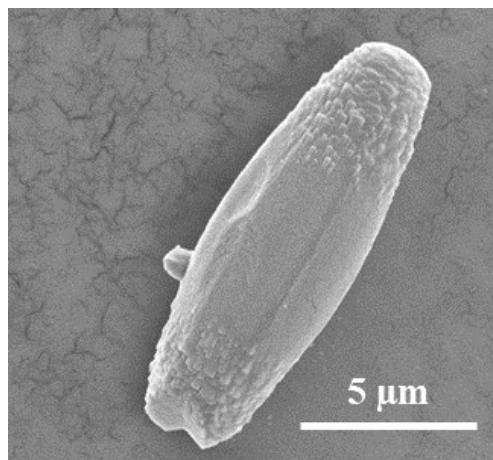


Figure S8. SEM micrograph of a single NU-1000-NH₂ particle.

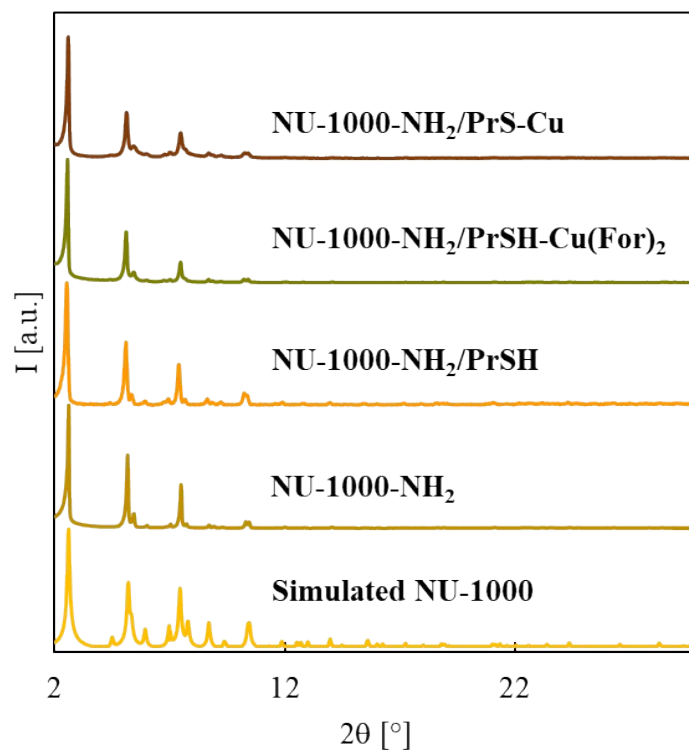


Figure S9. PXRD patterns of the studied powder samples compared with the simulated phase.

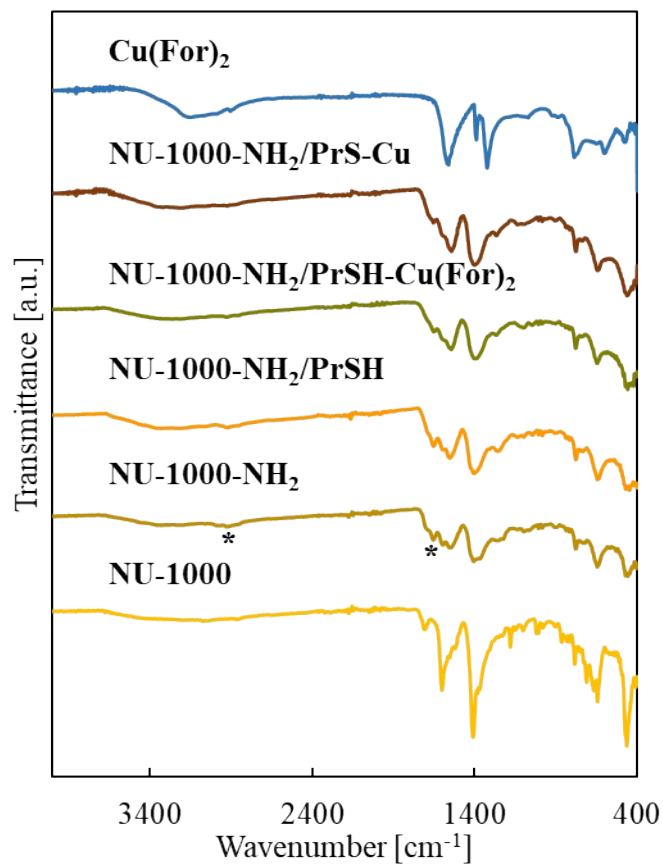


Figure S10. ATR-FTIR spectra of the studied samples compared to pristine NU-1000 and Cu(For)_2 . (*) indicates the bands associated to $-\text{NH}_2$ Fermi resonance and N-H bending at *ca.* 3000 and 1650 cm^{-1} , respectively, in the NU-1000- NH_2 sample.

Quantitative analysis of PrSH by $^1\text{H-NMR}$

$^1\text{H-NMR}$ was used to quantify the content of PrSH in NU-1000- NH_2/PrSH after sample digestion in hydrofluoric acid and further dissolution in DMSO-d_6 .² The molecular formula of NU-1000 contains 2 TBAPy- NH_2^{4+} ligands per 1 Zr_6 cluster. If the SALI substitution is completed, there should be 4 PrSH per 1 Zr_6 unit.³ Hence, when normalizing the integration peaks for one single molecule of $\text{H}_4\text{TBAPy-NH}_2$ in the $^1\text{H-NMR}$ spectra of the digested sample, the signals assigned to PrSH would show integration values two times higher in these spectra than in the one of the isolated PrSH compound (Fig. S11), if the four-fold PrSH substitution is accomplished. This is the case of the present study, showing a molecular ratio PrSH: $\text{H}_4\text{TBAPy-NH}_2$ of 2:1 (Fig. S12). Note that the peak assigned to proton (1) in PrSH (Fig. S11) is very sensitive to the electronic environment and shifts to lower values in the digested (Fig. S12) sample due to the deprotonation of the carboxylic acid.

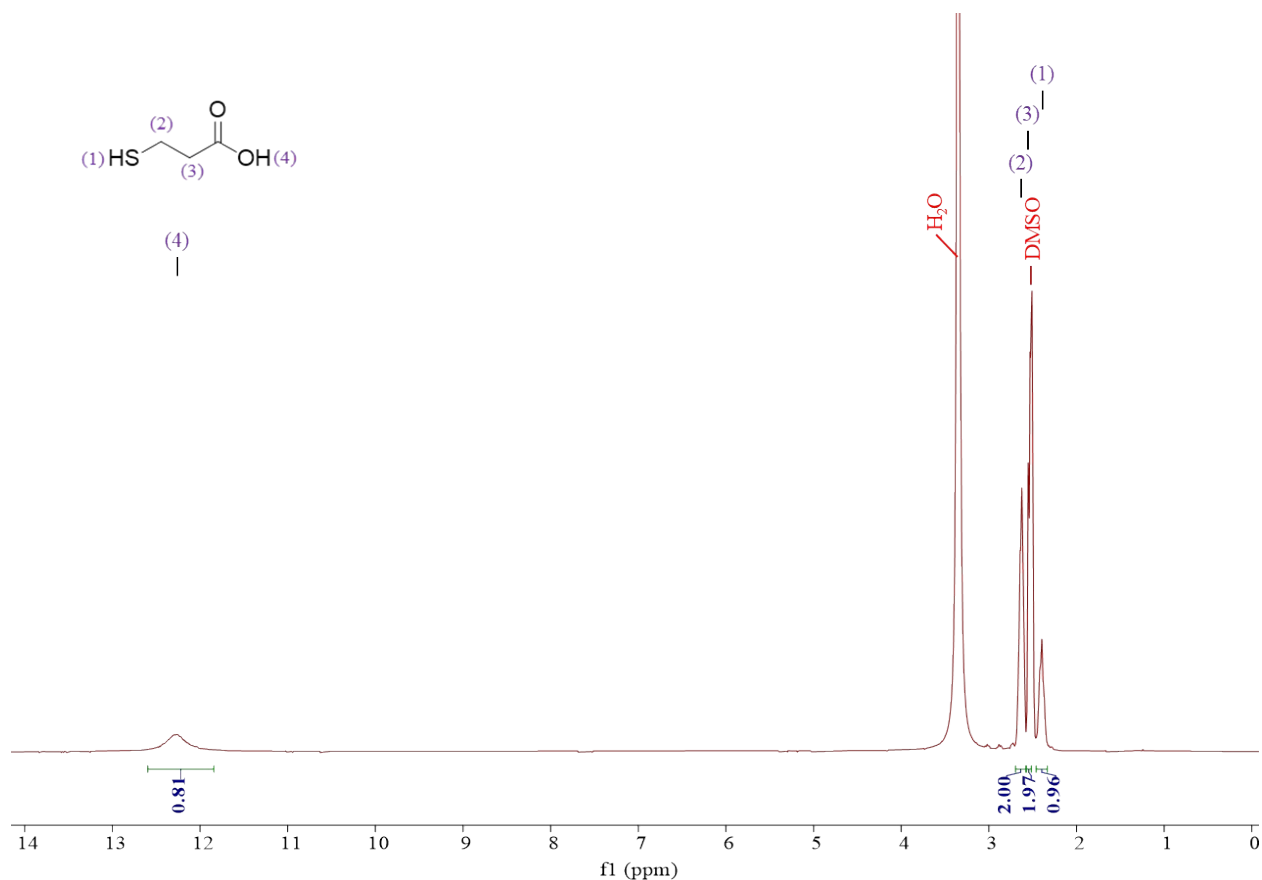


Figure S11. $^1\text{H-NMR}$ spectra of PrSH in DMSO-d_6 .

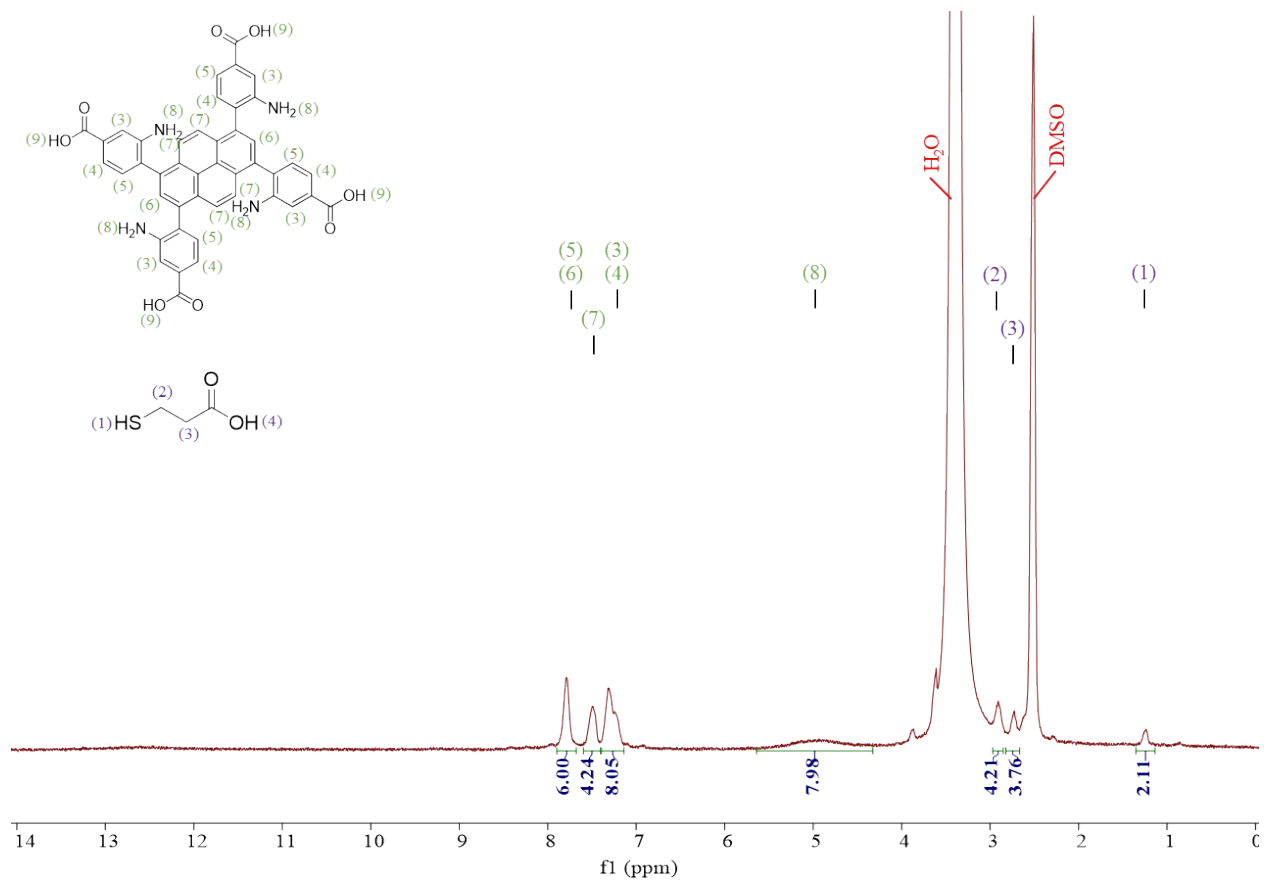


Figure S12. ¹H-NMR spectra of digested NU-1000-NH₂/PrSH in DMSO-d₆.

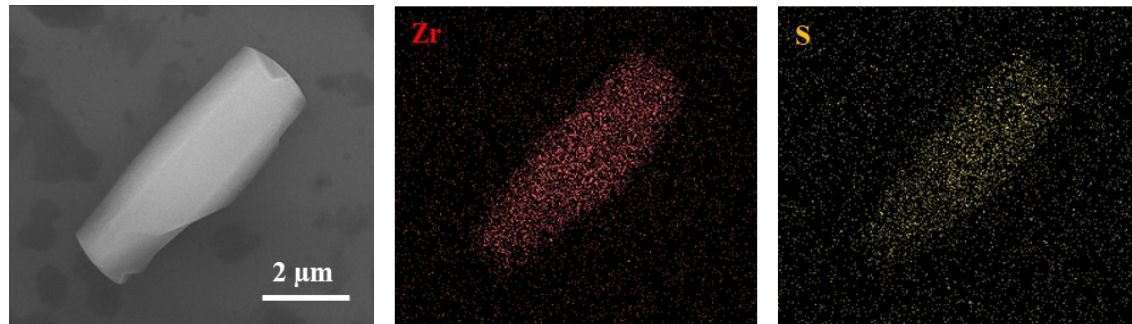


Figure S13. SEM image and EDS mapping of a NU-1000-NH₂/PrSH particle. Spots in red and yellow correspond to the elemental distribution of Zr and S, respectively.

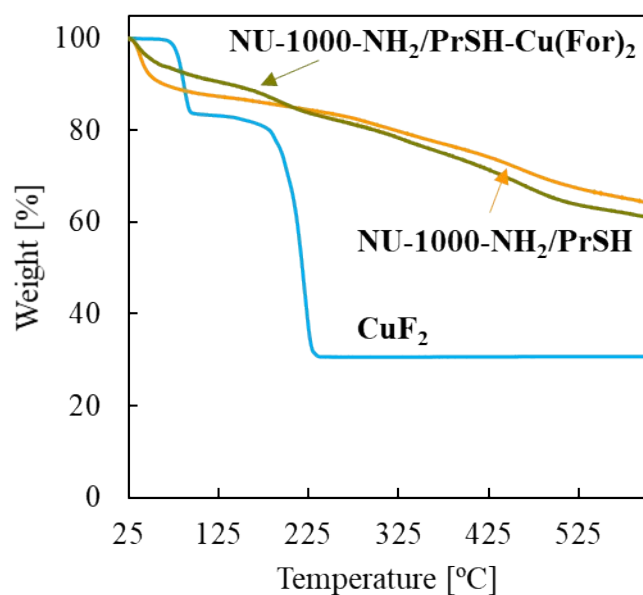


Figure S14. TGA analysis of NU-1000-NH₂/PrSH-Cu(For)₂ under H₂ (5 % in Ar) compared to the precursor materials.

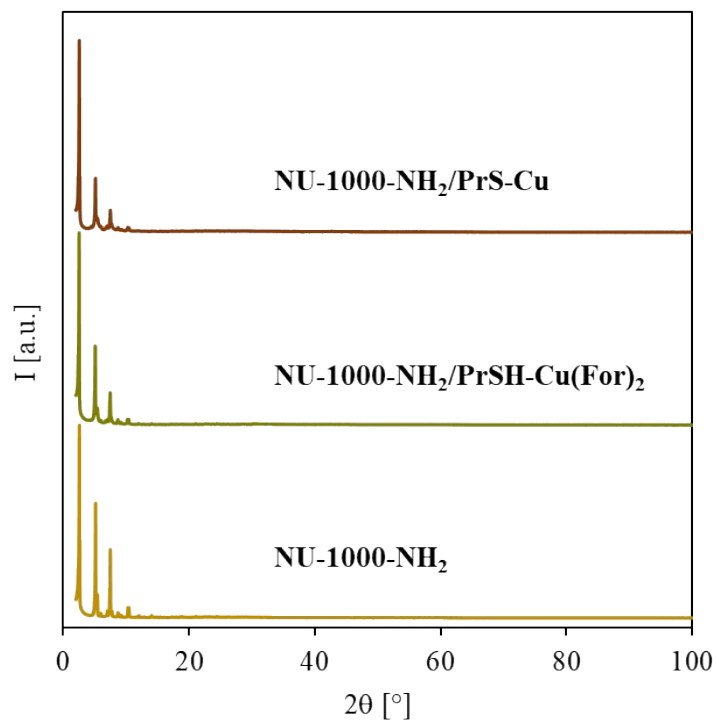


Figure S15. PXRD patterns of the studied powder samples at 2θ range from 2 to 100° .

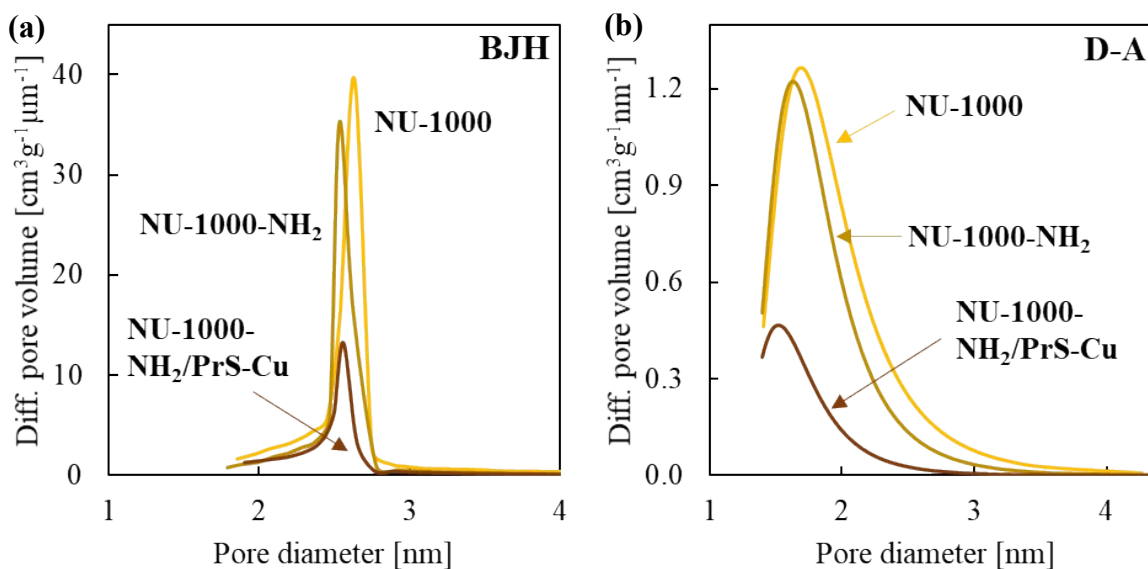


Figure S16. Pore size distribution of the studied samples according to (a) BJH and (b) D-A.

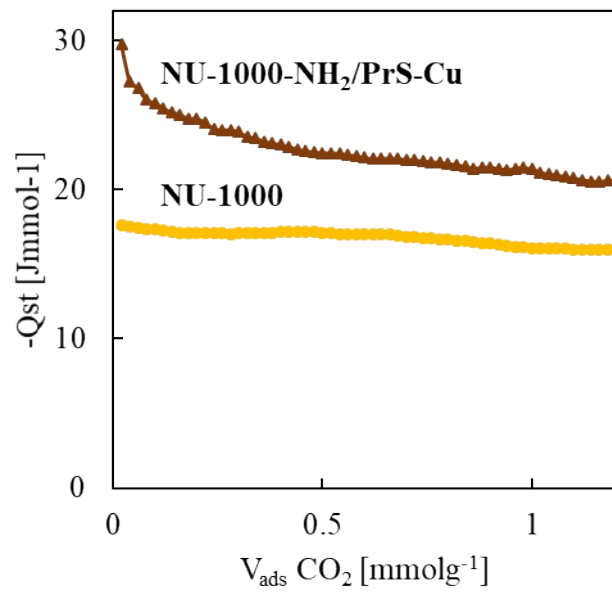


Figure S17. CO₂ enthalpy of adsorption (Q_{st}) of the studied samples.

Electrocatalysts characterization and results

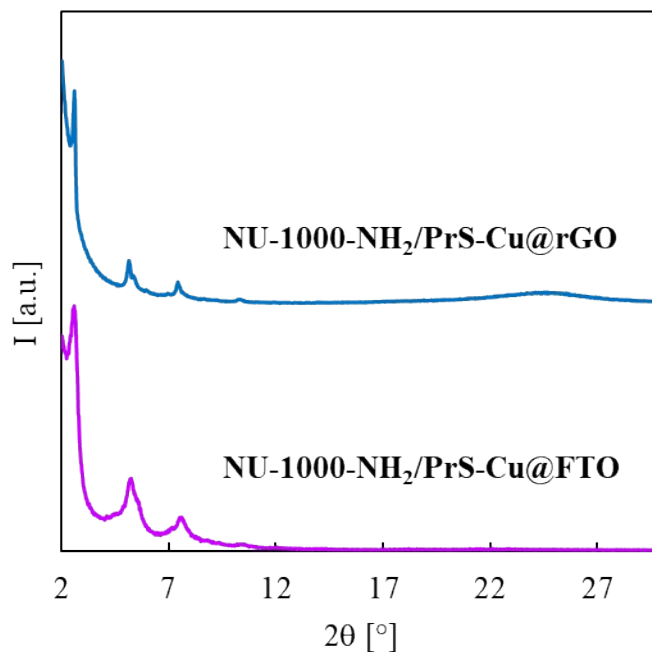


Figure S18. PXRD patterns of the studied working electrodes.

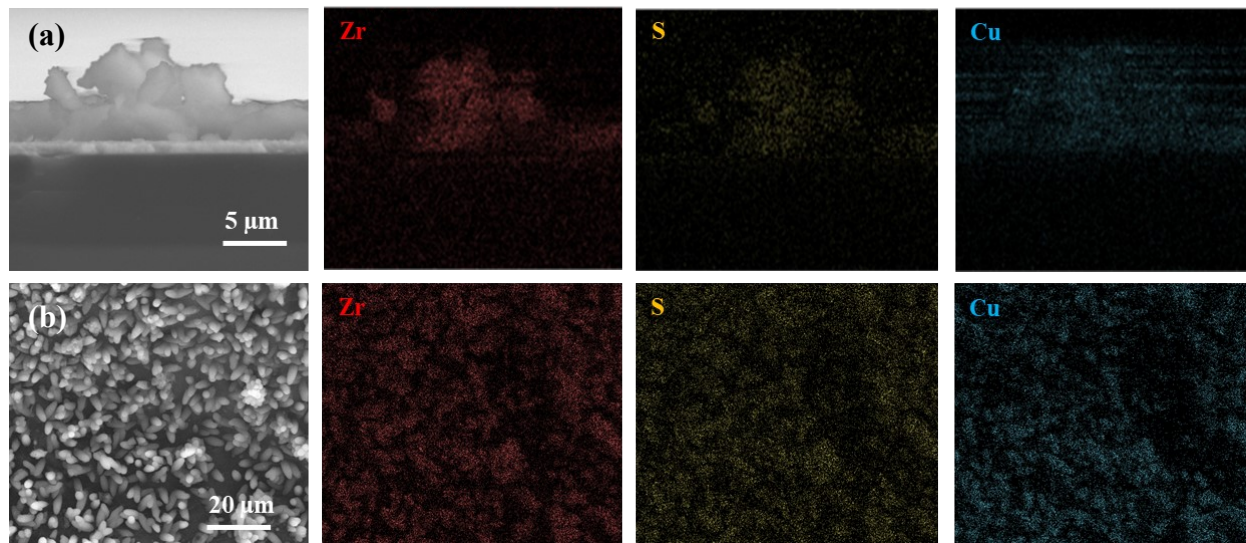


Figure S19. SEM image and EDS mapping of (a) NU-1000-NH₂/PrS-Cu@FTO (side-view) and (b) NU-1000-NH₂/PrS-Cu@rGO (top-view). Spots in red, yellow and blue correspond to the elemental distribution of Zr, S and Cu, respectively.

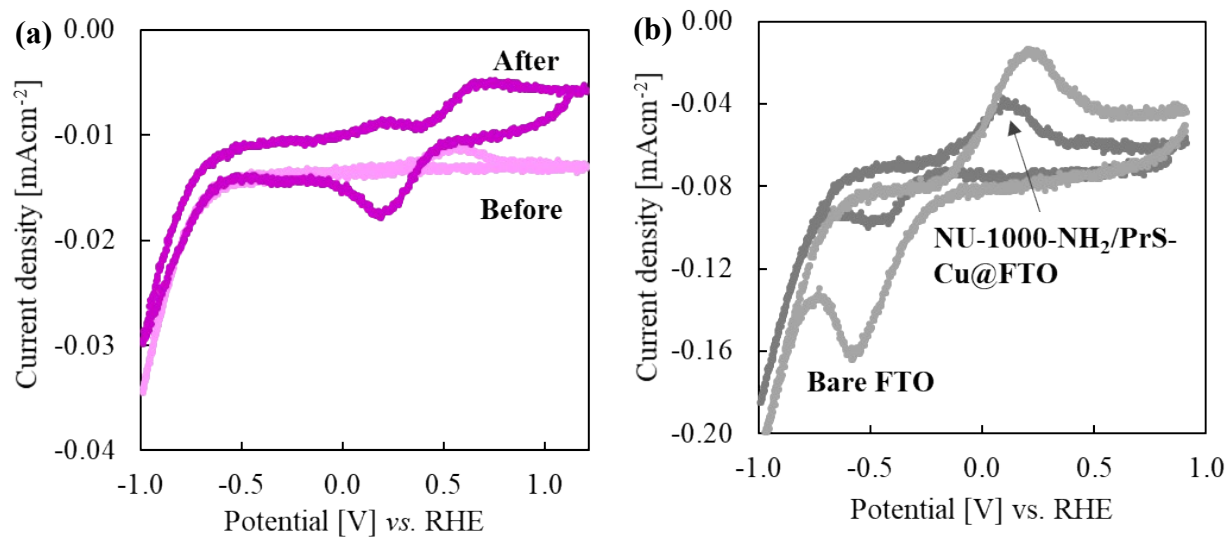


Figure S20. CV scan of (a) NU-1000-NH₂/PrS-Cu@FTO before and after electrochemical treatment at -0.6 V vs. RHE, and (b) bare FTO and NU-1000-NH₂/PrS-Cu@FTO after electrocatalytic testing at -0.8 V vs. RHE.

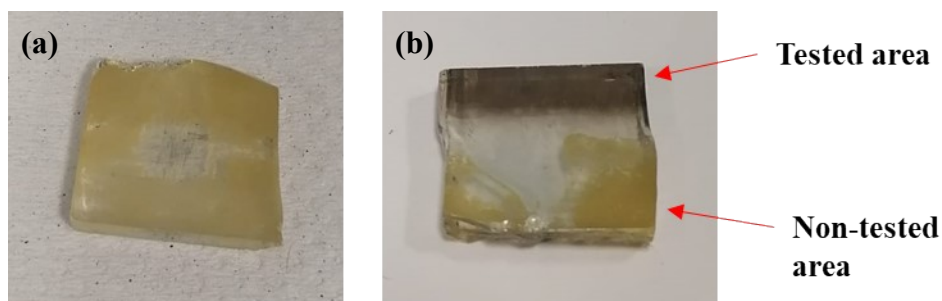


Figure S21. NU-1000-NH₂/PrS-Cu@FTO photograph (a) before and (b) after electrocatalytic testing (pointing at the tested and non-tested areas).

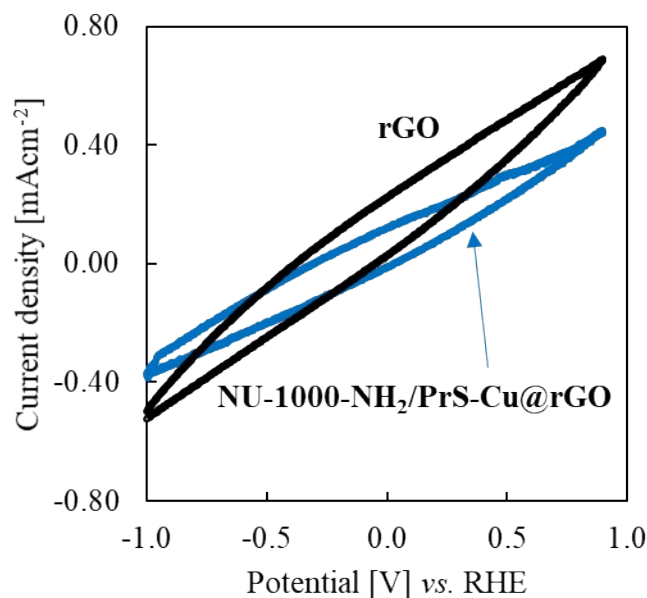


Figure S22. CV scan of (I) NU-1000-NH₂/PrS-Cu@rGO and (II) bare rGO after electrochemical treatment at -0.6 V vs. RHE.

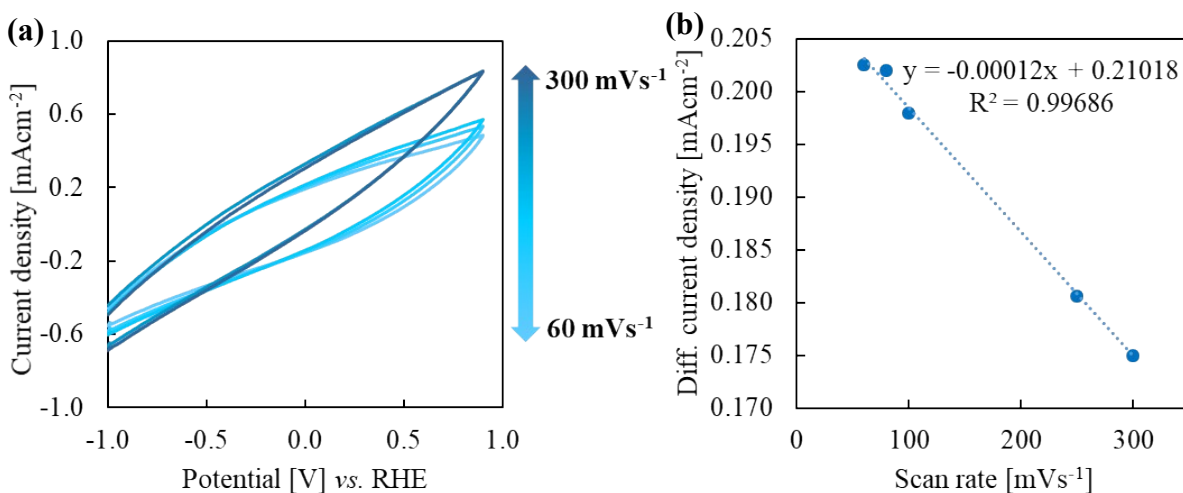


Figure S23. (a) CV scans of NU-1000-NH₂/PrS-Cu@rGO performed at several scan rates (60, 80, 100, 250 and 300 mVs⁻¹) and (b) differences in charging current density plotted against the studied scan rates (including the line equation).

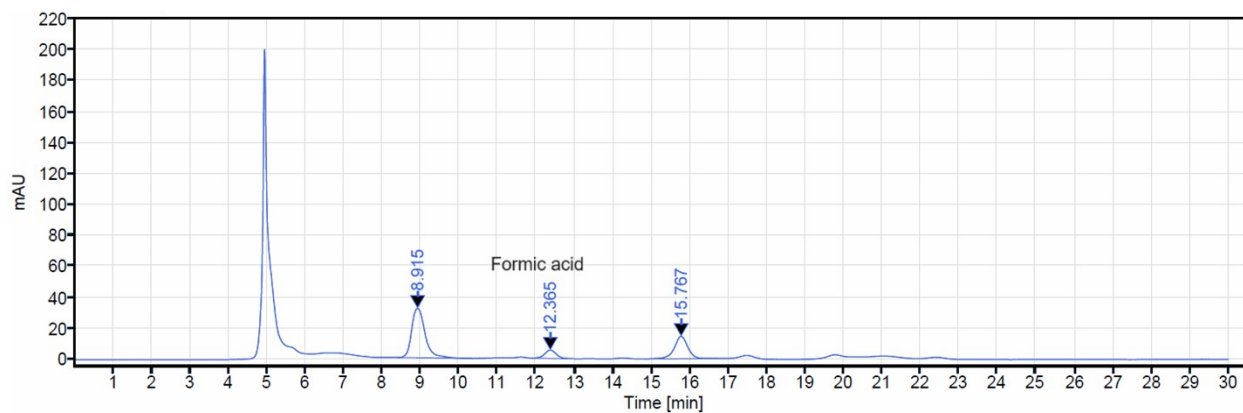


Figure S24. HPLC analysis of electrocatalysis with NU-1000-NH₂/PrS-Cu@rGO at -1.8 V vs. RHE.

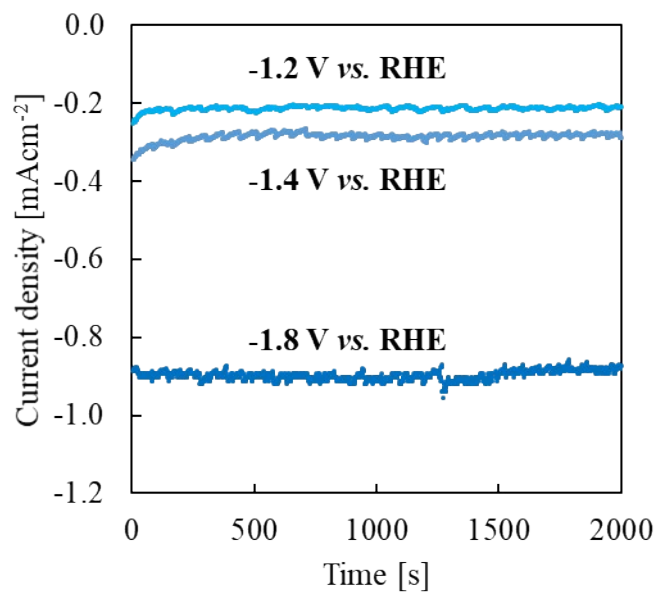


Figure S25. Chronoamperometric measurements of NU-1000-NH₂/PrS-Cu@rGO at different applied potentials over *ca.* 35 min.

References

- [1] T. Islamoglu, M.A. Ortuño, E. Proussaloglou, A.J. Howarth, N.A. Vermeulen, A. Atilgan, A.M. Asiri, C.J. Cramer, O.K. Farha, Presence versus proximity: the role of pendant amines in the catalytic hydrolysis of a nerve agent simulant, *Angew. Chem. Int. Ed.* 57 (2018) 1949-1953.
- [2] A. Rosado, O. Vallcorba, B. Vázquez-Lasa, L. García-Fernández, R.A. Ramírez-Jiménez, M.R. Aguilar, A.M. López-Periago, C. Domingo, J.A. Ayllón, Facile, fast and green synthesis of a highly porous calcium-syringate BioMOF with Intriguing triple bioactivity, *Inorg. Chem. Front.* 10 (2023) 2165–2173.
- [3] P. Deria, W. Bury, J. T. Hupp, Omar K. Farha, Versatile functionalization of the NU-1000 platform by solvent-assisted ligand incorporation, *Chem. Commun.* 50 (2014) 1965-1968.